

Immuno-oncological Efficacy of RXDX-106, a Novel TAM (TYRO3, AXL, MER) Family Small-Molecule Kinase Inhibitor



Yumi Yokoyama¹, Erin D. Lew¹, Ruth Seelige², Elizabeth A. Tindall³, Colin Walsh¹, Patrick C. Fagan¹, Jack Y. Lee¹, Robin Nevarez¹, Joanne Oh¹, Kathleen D. Tucker¹, Marissa Chen⁴, Amy Diliberto⁴, Heather Vaaler⁴, Kristen M. Smith⁴, Amanda Albert¹, Gary Li¹, and Jack D. Bui²

Abstract

Expression of the TAM (TYRO3, AXL, MER) family of receptor tyrosine kinases (RTK) has been associated with cancer progression, metastasis, and drug resistance. In immune cells, TAM RTKs can dampen inflammation in favor of homeostatic wound-healing responses, thus potentially contributing to the evasion of cancer cells from immune surveillance. Here we characterize the small-molecule RXDX-106 as a selective and potent pan-TAM RTK inhibitor with slow dissociation kinetics and significant antitumor activity in multiple syngeneic tumor models. Expression of AXL and MER on both immune and tumor cells increased during tumor progression. Tumor growth inhibition (TGI) following treatment with RXDX-106 was observed in wild-type mice and was abrogated in immunodeficient mice, suggesting that the antitumor activity of RXDX-106 is, in part, due to the presence of immune cells. RXDX-106-mediated TGI was associated with increased tumor-infiltrating leukocytes, M1-polarized intratumoral

macrophages, and activation of natural killer cells. RXDX-106 proportionally increased intratumoral CD8⁺ T cells and T-cell function as indicated by both IFN γ production and LCK phosphorylation (pY393). RXDX-106 exhibited its effects via direct actions on TAM RTKs expressed on intratumoral macrophages and dendritic cells, leading to indirect activation of other immune cells in the tumor. RXDX-106 also potentiated the effects of an immune checkpoint inhibitor, α -PD-1 Ab, resulting in enhanced antitumor efficacy and survival. Collectively, these results demonstrate the capacity of RXDX-106 to inhibit tumor growth and progression and suggest it may serve as an effective therapy against multiple tumor types.

Significance: The pan-TAM small-molecule kinase inhibitor RXDX-106 activates both innate and adaptive immunity to inhibit tumor growth and progression, indicating its clinical potential to treat a wide variety of cancers.

Introduction

Immune checkpoints can block cell expansion/activation, abrogate the immune response, and initiate return to homeostasis, but tumors have pathologically coopted these pathways to restrict effective antitumor responses (1). Targeted inhibition of these negative regulatory checkpoints has emerged as viable and

promising immunotherapies for cancer (2). Antibodies that block CTLA-4, PD-1, or PD-L1 show clinical efficacy by boosting CD4⁺ Th cells or by restoring activity of exhausted CD8⁺ T cells, respectively (3, 4). Nevertheless, the response rate to checkpoint blockade remains $\leq 30\%$ for many cancers, in part, due to the suppressive milieu in the tumor microenvironment (TME) stemming from suppressive innate immune cells, including myeloid-derived suppressor cells (MDSC; ref. 5), M2-like macrophages (6), dysfunctional dendritic cells (DC; ref. 7), and natural killer (NK) cells (8). Presumably, therapies that activate/polarize the innate immune system could synergize with checkpoint inhibitors to boost antitumor effects of the adaptive immune system (9).

One group of checkpoint molecules that regulate innate immunity are the TAM RTKs—TYRO3, AXL, and MER, which are broadly expressed on several immune cell lineages, including macrophages, DCs, and NK cells (10). With their ligands, GAS6 and PROS1, TAM RTKs help to resolve inflammatory signals and participate in wound healing. In *Mertk*^{-/-} mice, inefficient clearance of apoptotic cells by monocyte-derived and epithelial cells, a process dependent on MER activation by GAS6 or PROS1 complexed with externalized phosphatidylserine (PtdSer) on apoptotic bodies (11, 12), leads to aberrant accumulation of apoptotic material, instigating inflammation. MER also suppresses the M1 macrophage/pro-inflammatory cytokine response

¹Translational Research, Ignyta, Inc., San Diego, California. ²Department of Pathology, University of California, San Diego, La Jolla, California. ³Computational Biology, Ignyta, Inc., San Diego, California. ⁴Diagnostics, Ignyta, Inc., San Diego, California.

Note: Supplementary data for this article are available at Cancer Research Online (<http://cancerres.aacrjournals.org/>).

Y. Yokoyama, E.D. Lew, and R. Seelige contributed equally to this article.

E.A. Tindall and C. Walsh contributed equally to this article.

J.D. Bui and G. Li contributed equally to this article.

Corresponding Authors: Jack D. Bui, University of California, San Diego, 9500 Gilman Drive, La Jolla, CA 92093-0612. Phone: 858-534-3890; Fax: 858-822-5580; E-mail: jrbui@ucsd.edu; and Erin D. Lew, Ignyta, Inc., San Diego, CA 92121. Phone: 203-543-8260; Fax: 858-822-5580; E-mail: erindlew@gmail.com.

doi: 10.1158/0008-5472.CAN-18-2022

©2019 American Association for Cancer Research.

while enhancing the M2 macrophage/anti-inflammatory production (13–15). On antigen-presenting cells (APC), Toll-like receptor (TLR) signaling upregulates AXL, which complexes with the type-I interferon receptor (IFNAR1), eliciting negative feedback on further TLR signaling (16). In addition, activated CD8⁺ T cells upregulate PROS1 and externalize PtdSer; this complex, in turn, stimulates TAM receptors on APCs, reducing APC activity (17). Furthermore, TAM triple knockout mice (TAM TKO), although gestationally viable, develop chronic inflammation and systemic autoimmunity, multiple organ defects, and massive lymphoproliferative disease due to overactivation of the innate immune system and failure to clear apoptotic debris, leading to engagement of the adaptive immune response (18).

Abnormal overexpression of TAM RTKs and/or GAS6 has been documented in a wide range of malignancies (14, 19, 20). In contrast to its perceived inhibition of immune cell signaling, TAM receptor activation in tumor cells promotes survival and tumorigenicity (21, 22). In the TME, where resources such as oxygen and nutrients are scarce, TAM RTK signaling may be critical in providing survival cues (20, 23), while promoting chemoresistance, colony-forming potential, invasion/motility, and induction of epithelial-to-mesenchymal transition (EMT; refs. 14, 20, 21, 24). Thus, TAM RTKs may both dampen inflammation and activate/promote cancer cell progression, encouraging development of therapeutic agents that inhibit TAM receptors for cancer immunotherapy.

The frequent observation of ≥ 2 TAM RTKs coexpressed on immune cells (25) and the normal phenotype of single- or double-TAM knockout mice in contrast to the autoinflammatory and autoimmune phenotype of the TAM TKO (18), suggests a redundancy in TAM receptor activity in innate immune cells. Indeed, in response to selective TAM RTK agents (i.e., anti-AXL-specific inhibition), cancer cells upregulate other TAM RTK family members as a mechanism of resistance (26). In this report, we document the characterization of RXDX-106, a novel small-molecule inhibitor of all three TAM RTKs. RXDX-106 blocked TAM RTKs on both tumor and immune cells, both *in vitro* and *in vivo*. This activity reduced tumor progression, even in tumor cells that do not respond to TAM RTK inhibition, suggesting that RXDX-106 activated antitumor immunity. Indeed, RXDX-106 directly activated macrophages, leading to activation of NK and T cells, restoring tumor immunity. These results confirm the negative checkpoint activity of TAMs in tumor immunity and support the use of RXDX-106 to tip the immune rheostat in favor of an effective antitumor immune response.

Materials and Methods

Cell lines and reagents

Cell lines were purchased from Kerfast (MC38), Sigma-Aldrich (EMT-6), ATCC (CT26, NIH3T3), or DSMZ (Ba/F3), respectively, and maintained at \leq passage 10. Cell line authentication and pathogen testing was performed to confirm cell line identities and pathogen-free status (including *Mycoplasma* testing; IDEXX BioResearch). Micronized anhydrous free RXDX-106 (CEP-40783) was synthesized at Base Micro Technologies. Antibodies and qPCR primers utilized are listed in Supplementary Tables S1–S4.

In vivo studies

RXDX-106 *in vivo* oral dosing solution was made by suspending RXDX-106 in equal parts Oleic Acid (Thermo Fisher Scientific) and PEG400 (Sigma-Aldrich) at a concentration of 1 or 3 mg/mL,

and animals were dosed orally every day. Female C57BL/6, BALB/c, athymic nude, BALB/c nude, SCID Beige, and CD45.1 C57BL/6 mice between 6 and 7 weeks of age were ordered from Charles River. C57BL/6 MMTV-PyMT (PyMT) female mice were bred in-house [University of California, San Diego (UCSD), San Diego, CA]. CD45.1.2 C57BL/6 mice were a kind gift from Dr. John Chang (University of California, San Diego, San Diego, CA). Bones from *Axl*^{-/-} *Mertk*^{-/-} (AM) double knockout (AMdKO) mice were a kind gift from Dr. Greg Lemke (Salk Institute, La Jolla, CA). Animal experiments were conducted in accordance with guidelines established by the Explora Biolabs Institutional Animal Care Use Committee (IACUC; Igynta ACUP# EB15-050).

Cells (1×10^6 cells/mouse, unless otherwise indicated) were implanted subcutaneously on the right flank of each mouse. Tumor-bearing mice were randomized and treated orally every day with vehicle or RXDX-106 at 30 mg/kg or at indicated doses. For studies with NIH3T3 cells expressing TYRO3, AXL, and MER, SCID/Beige animals were inoculated and treated on the indicated day with RXDX-106 orally every day when mean tumor volume reached approximately 140, 60, and 150 mm³, respectively.

For TGI combination studies with anti-PD-1 antibody, MC38 and CT26 cells were implanted subcutaneously in the right flank of C57BL/6 and BALB/c mice, respectively. Mice were randomized and treated when tumors reached 130 mm³. Animals were treated with 30 mg/kg RXDX-106 (orally every day) \pm antibodies (intraperitoneally, two times/week; 10 mg/kg anti-PD-1 antibody or rat IgG2a antibodies). Survival was monitored for a maximum duration of 60 days or until tumor volume reached 2,000 mm³. Isotype antibody had no effect on tumor growth. For immunophenotyping and RNA-seq combination study, animals were treated for 7 days with either vehicle or RXDX-106 (orally every day) \pm antibodies (anti-PD-1 antibody or rat IgG2a antibodies (10 mg/kg) intraperitoneally 2 \times /week. PyMT mice were treated orally every day with vehicle or RXDX-106 at 30 mg/kg at tumor onset.

Generation of bone marrow chimeric mice

Eight-week-old female CD45.1 mice were irradiated with 1,000 cGy and intravenously injected with 5×10^6 bone marrow (BM) cells from WT CD45.2 or AMdKO CD45.2, respectively. For some experiments, CD45.1 mice were intravenously injected with bone marrow cells from WT CD45.1.2 and AMdKO CD45.2 at a 1:1 ratio. Proper reconstitution was tested by FACS analysis of cheek blood after 6 weeks.

In vivo proliferation determined by BrdU incorporation

Mice were subcutaneously inoculated with 1×10^5 MC38/mouse and treated with 30 mg/kg RXDX-106 (or vehicle) for 1 week after tumors reached a size of 400 mm³. Forty-eight and 24 hours before harvest, mice were intraperitoneally injected with 1 mg of BrdU/mouse (eBioscience). Tumor-draining lymph nodes (LN) and tumors were harvested and single-cell suspensions were stained for BrdU expression after DNase treatment according to the manufacturer's protocol. Samples were analyzed by FACS. Differences shown are not significant. Animals were housed in the UCSD Animal Care Facility, and all experiments were conducted in accordance with guidelines established by the UCSD IACUC (protocol #S06201).

Immunophenotypical analysis

For immunophenotyping, MC38 tumor-bearing mice were dosed orally every day with vehicle or RXDX-106 for 7 days or

as indicated. Dissociated tumor cells were washed with PBS, stained with Fixable Viability Stain 780 (BD Biosciences) for 30 minutes at 4°C, and washed with FACS staining buffer. Cells were blocked with Mouse FcR Blocking Reagent (Miltenyi Biotec) prior to staining, and then cells were stained with antibodies for 30 minutes at 4°C. After washing with FACS buffer, cells were fixed with 1% paraformaldehyde. For intracellular staining of FoxP3 and IFN γ , Foxp3/Transcription Factor Staining Buffer Set (eBioscience) was used following the manufacturer's instructions. For detection of intracellular phospho-TAM, tumors were collected and dissociated with 1 mmol/L Na₃VO₄. Cells were first stained for surface markers, permeabilized with BD Cytotfix/Cytoperm, and stained with phospho-TAM antibodies. Samples were acquired on BD FACS Celesta flow cytometer (BD Biosciences) and data analyzed with FlowJo software.

Statistical analysis

Statistical analysis was done either by ANOVA or two-tailed *t* test using GraphPad Prism (version 6.07; GraphPad Software, Inc.). *, *P* (*t* test) or FDR <0.05; **, *P* or FDR <0.01; ***, *P* or FDR <0.001; ****, *P* or FDR <0.0001.

Results

RXDX-106 is a pan-TAM RTK small-molecule inhibitor

The overexpression of multiple TAM receptors has been implicated in driving tumor growth and metastasis across multiple cancer types (14, 27). In addition, there is evidence of coexpression and functional redundancy of the receptors on immune cell types including macrophages, NK, and T cells (28–30). Hence, we developed RXDX-106, a small molecule, ATP-competitive inhibitor that targets all three TAM receptors. RXDX-106 bound to the kinase domains corresponding to TYRO3, AXL, and MER with an IC₅₀ of 3.50, 0.69, and 1.89 nmol/L, respectively (Fig. 1A). In a broader activity-based kinase screen, we found that RXDX-106 is highly selective for the TAM RTKs with additional activity against the highly related c-MET/RON families (Supplementary Fig. S1A). Notably, RXDX-106 had slow dissociation kinetics indicative of a type II mode of inhibition (31) and remained bound to the TAM RTK targets at least 5-fold longer than other TAM RTK inhibitors tested (Supplementary Fig. S1B and S1C), suggesting more durable *in vivo* pharmacodynamics (32).

To corroborate the biochemical assays, target engagement of RXDX-106 was measured in NIH3T3 cells expressing human TYRO3, AXL, or MER. Receptor activation and signal transduction were dose-dependently inhibited by RXDX-106 with low nanomolar cellular IC₅₀s (Fig. 1B). Similarly, in a Ba/F3 cell line dependent on the ectopic expression of human AXL expression for cellular survival upon IL3 withdrawal, RXDX-106 inhibited cellular proliferation and viability with an IC₅₀ of 0.31 nmol/L (Supplementary Fig. S1D). RXDX-106 also inhibited mouse TAM RTKs. In bone marrow–derived or peritoneal macrophages polarized with polyI:C or dexamethasone to express either AXL or MER, respectively, we observed dose-dependent inhibition of GAS6-dependent cellular signaling and inhibition of TAM RTK–dependent phagocytosis, a known readout for TAM RTK function (Supplementary Fig. S1E and S1F; refs. 30, 33).

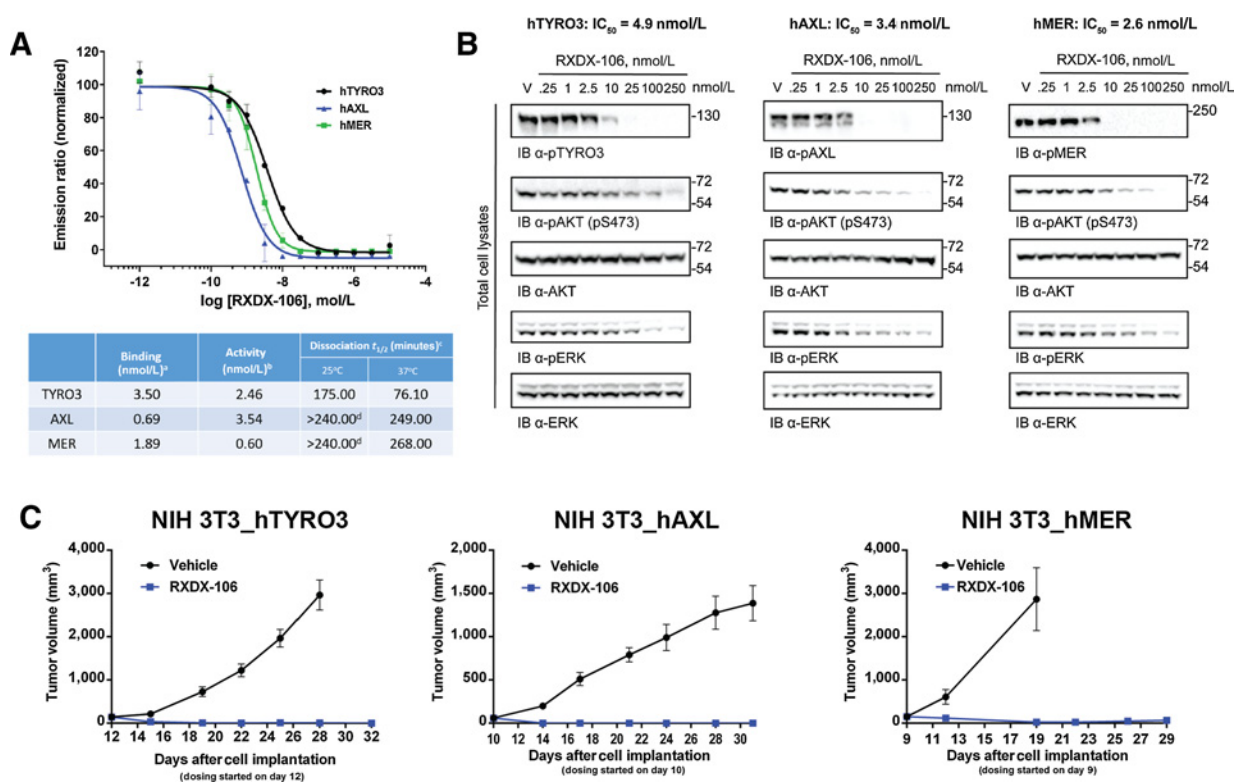
We next investigated RXDX-106 efficacy *in vivo* using a classic transformation assay with NIH3T3 cells transduced with human TYRO3, AXL, or MER, allowing them to form tumors in mice (19, 34, 35). Mice implanted with NIH3T3_TYRO3, AXL, or MER cell

lines treated with RXDX-106 showed rapid tumor regression, demonstrating *in vivo* efficacy of RXDX-106 (Fig. 1C). In a more physiologic *in vivo* setting, RXDX-106 inhibited the growth of primary mouse mammary tumors driven by oncogenic expression of the middle T antigen from polyoma virus (PyMT) in mammary tissues, although the differences were not significant due to control group variability (Supplementary Fig. S1G).

RXDX-106 efficacy is mediated by immunomodulatory function

TAM RTKs play key roles in both survival of tumor cells and in negative regulation of immune cell function. To determine whether RXDX-106 exerts its actions by targeting TAM RTKs directly on tumor cells or via immune cells, we compared the TGI of RXDX-106 in immunocompetent versus immunodeficient mice in three syngeneic mouse models. RXDX-106 significantly promoted TGI in the immunocompetent mice, whereas the effect in immunodeficient mice was not significant. Specifically, the TGI in the MC38 model was 61% (*P* = 0.016) in C57BL/6 versus 22% in athymic nude mice at day 18 (Fig. 2A). TGI in the Renca model was 60% (*P* < 0.0001) in BALB/c versus 19% in BALB/c nude mice at day 21 (Fig. 2B). The TGI in the EMT-6 model was 74% (*P* = 0.023) in BALB/c versus 17% in BALB/c nude mice at day 15 (Fig. 2C).

To investigate the effect of RXDX-106 on immune cells in the TME, MC38 tumor-bearing mice were treated with 1, 3, 10, 30, and 60 mg/kg RXDX-106 for 7 days (Fig. 2D, top), and CD45⁺ TILs were measured by flow cytometry. A significant dose-dependent increase in TILs was observed with RXDX-106 (Fig. 2E), suggesting that RXDX-106 increased immune cell recruitment, survival, or proliferation in the TME. In addition, in a timecourse assay (Fig. 2D, bottom), this increase in immune cell infiltration was significant by day 5 (Fig. 2F) and at the transcript level by day 3 post-RXDX-106 as indicated by an increase in *Ptprc* (CD45) gene expression in the TME by RNA-seq that continued through day 9 (Fig. 2G). Notably, genes induced in the TME posttreatment with RXDX-106 were almost exclusively involved in immune function, as demonstrated by an unbiased global gene ontology analysis (GO) in which 16 of the top 20 gene pathways induced by RXDX-106 were immune-related (Fig. 2H; Supplementary Table S5). To further elucidate the significance of the immune system in mediating RXDX-106–induced TGI and to investigate the impact of other kinases inhibited by RXDX-106 (Supplementary Fig. S1A), we generated bone marrow chimeric mice by irradiation and reconstitution with bone marrow from either WT or *Axl*^{−/−}*Mertk*^{−/−} double-knockout mice (hereafter WT BM or AMdKO BM) and transplanted them with MC38 cells (Fig. 2I). Reconstitution was >90% in all mice. We found no difference in tumor growth between WT and AMdKO BM mice at the basal state (Fig. 2J). In line with publications on AMdKO mice (18), we observed a hyperactivation of some immune cells in the spleen of AMdKO BM mice, represented by more MHCII^{hi} macrophages and CD44⁺CD4⁺ and CD8⁺ T cells (Fig. 2K). However, this hyperactivation did not transfer to the TME, in part, explaining why there was no TGI in MC38-challenged AMdKO BM mice. We also observed no difference in the number of MDSCs in the tumor (Supplementary Fig. S5E). Importantly, RXDX-106 was not able to inhibit tumor growth in the AMdKO BM mice (in contrast with WT BM mice; ref. Fig. 2J), suggesting that not only is its effect on TGI immune-mediated, but also that it solely acts on AXL and MER on immune cells. TYRO3, c-MET, RON, or other kinases that

**Figure 1.**

RXDX-106 is a pan-TAM RTK inhibitor with durable target inhibition. **A**, Top, LanthaScreen equilibrium binding was performed and biochemical binding IC₅₀ for TYRO3, AXL, and MER was determined. (bottom). Table shows calculated biochemical parameters for RXDX-106 as determined by LanthaScreen Kinase: ^aBinding and ^bRadiometric Kinase Activity Assay and ^cDissociation Assay. ^dDetermination limited to 4-hours due to signal decay. **B**, *In vitro* inhibition in NIH3T3 cells expressing human TAM RTKs. **C**, RXDX-106 mediates tumor regression in SCID/Beige mice harboring NIH3T3_TYRO3, AXL, or MER tumors, respectively. *n* = 10 mice/group.

RXDX-106 can inhibit (Supplementary Fig. S1A) do not seem to play a significant role in RXDX-106-mediated TGI.

RXDX-106 directly affects TAM RTK signaling *in vivo* on immune cells

Our data thus far suggest that RXDX-106 requires immune cells *in vivo* to mediate antitumor responses. Because TAMs are expressed on both tumor and immune cells, we sought to investigate whether RXDX-106 could directly kill tumor cells, leading indirectly to immune cell activation. We therefore examined the effect of RXDX-106 on tumor cell viability *in vitro*. Fig. 3A shows that RXDX-106 was more than 100-fold less potent (IC₅₀ = 2.67 μmol/L) than staurosporine in killing MC38 cells, with an IC₅₀ that is 1,000× higher than the IC₅₀ to block *in vitro* TAM RTK kinase activity (Fig. 1B). Proliferation of tumor cells *in vivo*, as measured by Ki67, was also not affected by RXDX-106 (Fig. 3B; Supplementary Fig. S2A), suggesting that RXDX-106's antitumor effect was mediated by an immune response instead of direct antiproliferative activity on the cancer cell.

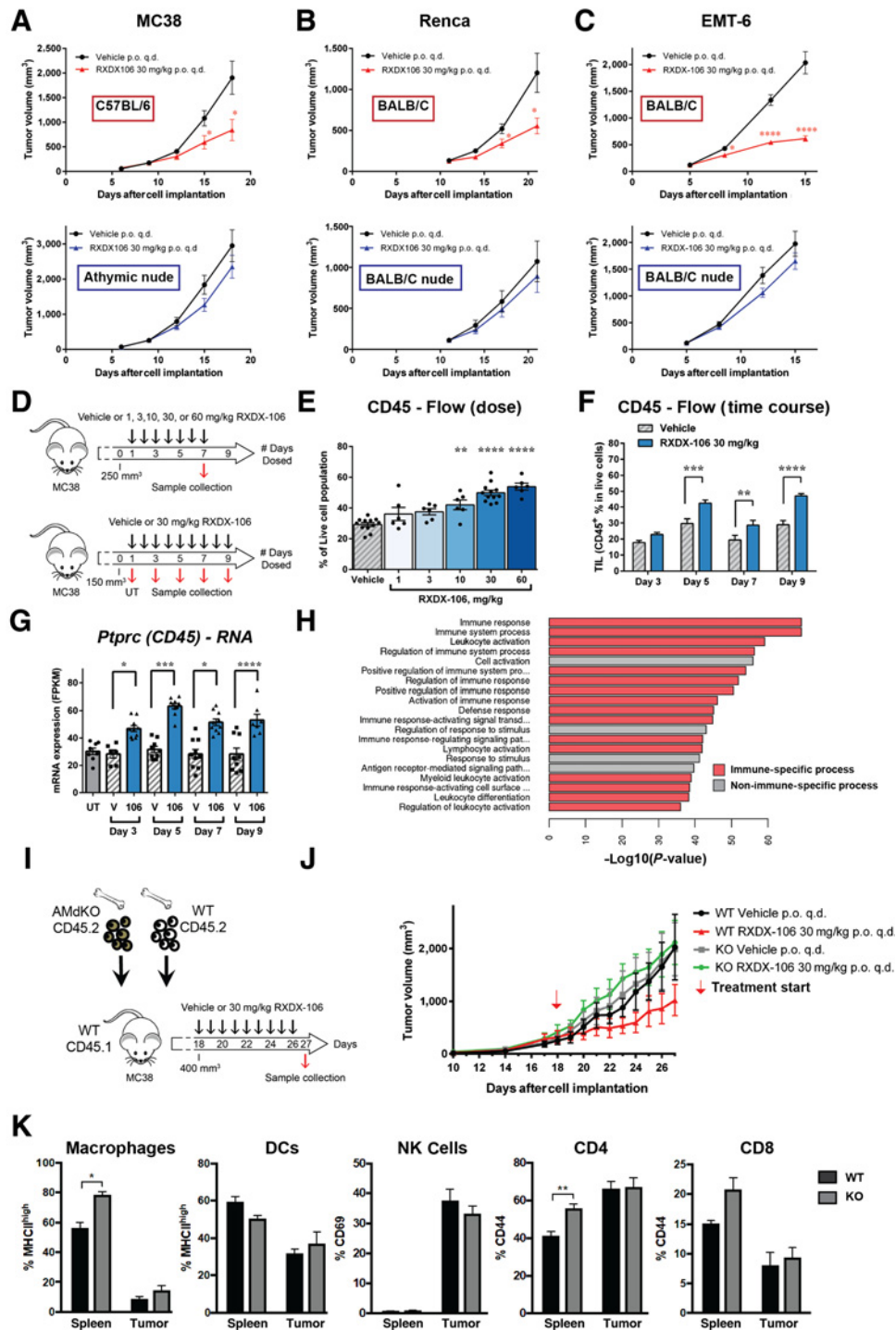
We next examined the expression of TAM RTKs on tumor versus immune cells *in vivo*. During tumor progression, an increase in cell surface MER was observed on both tumor cells and tumor-associated macrophages (TAMφ; CD11b^{hi}Ly6G^{lo}Ly6C^{lo}F4/80^{hi}) by flow cytometry, with a more significant increase observed on TAMφ (Fig. 3C; Supplementary Fig. S2B). This increase in expression was specific for TAMφ, because it was not seen on mMDSCs

and gMDSCs (36). A further increase in overall MER levels in the TME was observed in tumor samples of RXDX-106-treated animals (Fig. 3D), most likely due to drug-mediated increases in TILs as RNA-seq analysis of F4/80⁺, CD49b⁺, and CD90.2⁺-depleted tumor samples did not have increases in *Mertk* gene expression with RXDX-106 and only the CD45⁺ population had detectable MER expression by Western blot analysis (Supplementary Fig. S2C and S2D). Similarly, a dose-dependent increase in *Mertk* gene expression was observed by RNA-seq analysis of whole tumors, in agreement with RXDX-106-mediated increases in MER-expressing TILs (Supplementary Fig. S2E). Notably, despite these increases in TAM RTK expression, a striking decrease in AXL and MER but not TYRO3 phosphorylation was observed, demonstrating the potent inhibitory effect of RXDX-106 in the TME (Fig. 3E and F). Inhibition of TAM RTKs by RXDX-106 occurred on both the MC38 tumor cells and TAMφ, as demonstrated by a decrease in phosphorylated TAM RTKs (pY779) in both MHCII^{hi} and MHCII^{lo} macrophage populations and on tumor cells (Fig. 3G; Supplementary Fig. S2F).

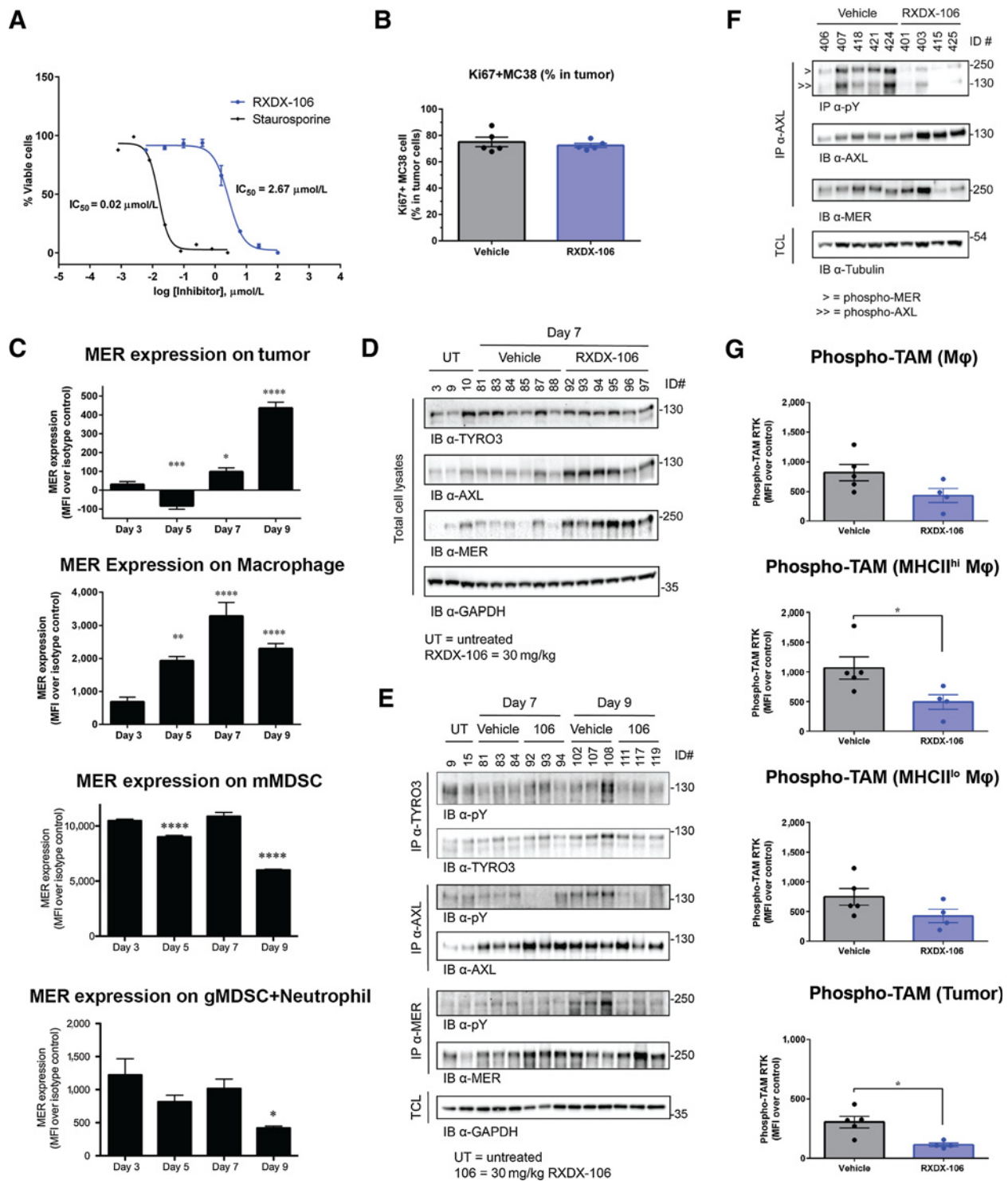
RXDX-106 increases innate immune responses to mediate antitumor effects

To further elucidate the cell types activated by RXDX-106 in the TME, immunophenotyping was performed on MC38 TILs from animals treated for 7 days with vehicle or RXDX-106 once mean tumor size reached 400 mm³ (Supplementary Fig. S3A; Fig. 4A).

Yokoyama et al.

**Figure 2.**

RXDX-106 induces immune-mediated antitumor activity. MC38 (A), Renca (B), EMT6 tumor models in immunocompetent (top) or immunodeficient (bottom) mice (C). Treatment started post-randomization when tumor size reached approximately 200 mm³ (MC38) or 120 mm³ (Renca and EMT6). D, Schematic illustrating *in vivo* dosing/sample collection for dose escalation (top) or timecourse (bottom), respectively. Black arrows, dosing; red arrows, sample collection 2 hours post-dosing; UT, sample collection prior to treatment. E, CD45⁺ population in MC38-tumor-bearing animals treated with 1, 3, 10, 30, or 60 mg/kg of RXDX-106 for 7 days. F and G, Whole tumor global gene and protein modulations by flow cytometry (F) and RNA-seq (G) in MC38 tumor-bearing animals treated for 3, 5, 7, or 9 days with 30 mg/kg RXDX-106. H, GO enrichment analysis with $-\log_{10} P$ values of top 20 GO terms enriched for differentially expressed genes (defined as $\log_2 FC > 1$, FDR < 0.01 , and FPKM > 1 in ≥ 2 mice) at day 5. Red bars, immune-related pathways; $n = 10$. I and J, Lethally irradiated CD45.1 mice transplanted with BM from CD45.2 WT or AMdKO were challenged with MC38 and tumor growth monitored post-treatment. K, Percentages of MHCII^{hi} macrophages and DCs; CD69⁺ of NK cells; CD44⁺ of CD4⁺ and CD8⁺ T cells in the spleens and tumors; $n = 5$. Data are mean \pm SEM. * $P < 0.05$; ** $P < 0.01$; *** $P < 0.001$; **** $P < 0.0001$.

**Figure 3.**

RXDX-106 directly affects TAM RTKs on immune cells *in vivo*. **A**, *In vitro* cell viability assay in MC38 cells treated with RXDX-106 or staurosporine for 72 hours. **B–G**, Tumors from MC38 tumor-bearing mice were collected and analyzed for RXDX-106 effects on tumor cell proliferation and TAM RTK activation as illustrated in Fig. 2D (bottom). **B**, *In vivo* effect of RXDX-106 on tumor cell proliferation (CD45⁺ Ki67⁺) by flow cytometry. **C**, TAM RTK expression on MC38 tumors (CD45⁺), TAM ϕ -CD11b^{hi}Ly6G^{lo}Ly6C^{lo}F4/80^{hi}, mMDSCs-CD11b^{hi}Ly6G^{lo}Ly6C^{hi}, and gMDSCs/Neutrophils-CD11b^{hi}Ly6G^{hi}Ly6C^{lo} during tumor progression. Statistical analysis relative to day 3. **D** and **E**, *Ex vivo* analysis of TAM RTK protein expression (**D**) and TAM RTK activation (**E**) in MC38 TME. **F** and **G**, Phosphorylation status of TAM RTKs in MC38 tumors 7-day posttreatment assessed in parallel by Western blot analysis (**F**) and flow cytometry (**G**). Data are mean \pm SEM; $n = 8–10$. *, $P < 0.05$; **, $P < 0.01$; ***, $P < 0.001$; ****, $P < 0.0001$.

Consistent with previous experiments (Fig. 2), RXDX-106 significantly mediated TGI (Fig. 4B) and increased TILs (Vehicle: 21.32% vs. RXDX-106: 38.41% in total live cells, $P < 0.0001$; Fig. 4C), with a striking increase in the percentage of macrophages (vehicle: 7.43% vs. RXDX-106: 16.78% in total live, $P < 0.0001$; Fig. 4D). In addition, there was a dramatic increase in MHCII^{hi} (M1-like) macrophages (vehicle: 18.45% vs. RXDX-106: 38.88% in macrophages, $P < 0.0001$; Fig. 4E) and a significant decrease in MHCII^{lo} (M2-like) macrophages (vehicle: 16.15% vs. RXDX-106: 5.78% in macrophages, $P < 0.0001$; Fig. 4F), resulting in overall polarization of macrophages to an M1-like/antitumorigenic phenotype (Fig. 4G).

In addition to an increase in MHCII^{hi} macrophages, there was also a significant increase in NK cells in the TME (Fig. 4H). *Ex vivo* reactivation of NK cells in tumors with IL12/IL18/anti-NK1.1 Ab revealed significant activation of NK cells by RXDX-106 as demonstrated by increased IFN γ ⁺ NK cells from 67.8% (vehicle) to 76.0% (RXDX-106; $P = 0.047$; Fig. 4I). These phenotypic changes were also reflected at the transcriptional level, as transcripts associated with macrophages (F4/80⁺) and NK cells (CD49b⁺) were enriched in dissociated tumors. Moreover, in macrophages, RXDX-106 decreased M2-related genes, *Arg1*, *Fizz1*, and *Ym-1* and increased MHCII-related genes, *Ciita* and *H2-Ab*, and *Siglec1* (Fig. 4J). In NK cells, the activation genes *Tnfa*, *Cd69*, *Klrg1*, *Il2ra*, *Ifng*, and *Zbtb32* were increased by RXDX-106 (Fig. 4K). In addition, VEGF transcript and protein were significantly reduced in a dose-dependent manner throughout the study (day 3–9 posttreatment; Supplementary Fig. S3B–S3D), further indicating innate immune modulation. No significant changes in MDSCs or neutrophils were observed in the TME by RXDX-106 (Supplementary Fig. S3E). Finally, activation of innate cells correlated with activation of adaptive immunity, because in the same experiments, IFN γ production by CD8⁺ and CD4⁺ T cells was increased post-RXDX-106 treatment (Fig. 4L–N). In addition, increases in TNF α , FasL, IFN γ , and GranzymeB in tumor cell lysates and increases in PD-1 on CD8⁺ T cells were observed with RXDX-106 (Supplementary Fig. S4A–S4E). These cytokine modulations and changes in overall immune cell numbers were largely undetectable in peripheral blood, indicating that the effects, mediated by RXDX-106, were limited to the TME (Supplementary Fig. S4F).

RXDX-106 enhances adaptive immune response via cell-extrinsic mechanisms

In addition to their role in modulating the innate immune response, TAM RTKs can also modulate activity of adaptive immune cells like T cells (37, 38). Therefore, we examined the effect of RXDX-106 on the adaptive immune response. Mice were inoculated with MC38 cells such that the growth rate of the tumor was slower relative to Fig. 4 (Fig. 5A and B). We found that RXDX-106 significantly induced the accumulation of CD8⁺ but not total CD4⁺ cells or Tregs in the tumor (Fig. 5C–E). The increase in CD8⁺ cells ($P = 0.0036$) was likely due to enhanced proliferation because we found increased Ki-67⁺CD8⁺ T cells after RXDX-106 treatment ($P = 0.0065$; Fig. 5F). PD-1 expression and LCK phosphorylation (pY393) were both enhanced compared with vehicle treatment (Fig. 5G and H), suggesting that there might be increased signal transduction via the TCR.

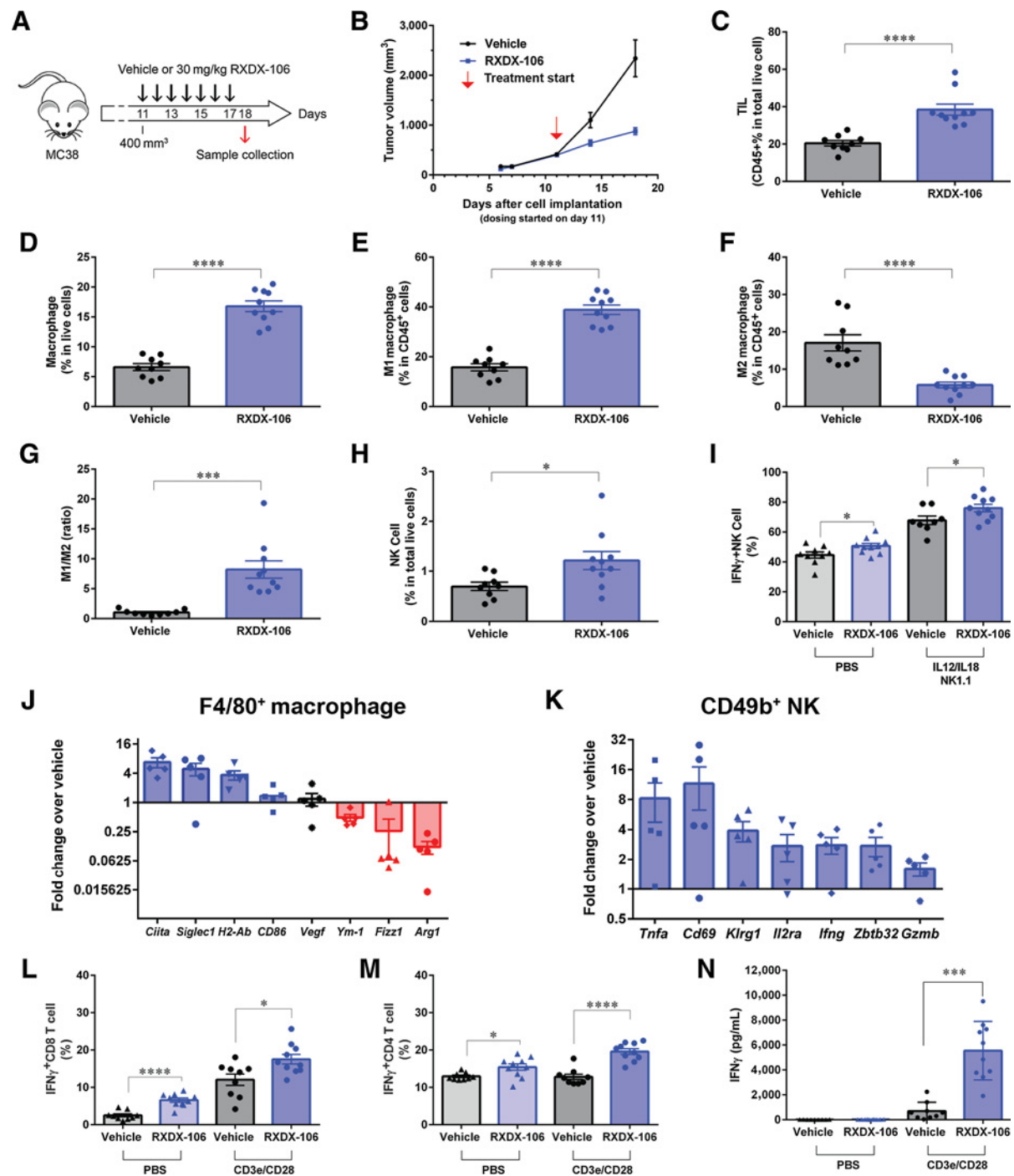
To further determine the cell type directly affected by RXDX-106 and to better assess cell-intrinsic roles for TAM RTKs, we generated mixed bone marrow chimeric mice reconstituted with a 1:1 mixture of bone marrow from WT:*Axl*^{-/-}*Mertk*^{-/-} (AMdKO)

mice and treated them with RXDX-106 for 1 week after MC38 tumor establishment (Fig. 5I and J; Supplementary Fig. S5A). We reasoned that comparing KO with WT cells would inform us whether the inhibitor activated any immune cell type directly, in which case, the impact of RXDX-106 would be to activate WT cells and have no impact on KO cells. We first examined the reconstitution of WT and AMdKO cells in the tumor in the absence of RXDX-106. Fig. 5K shows that AMdKO macrophages and DCs reconstituted the tumor (but not the LN) better than WT macrophages and DCs, indicating a clear cell-intrinsic activity for TAM RTKs on myeloid cells in the absence of RXDX-106. Notably, this did not occur with T or NK cells, suggesting that TAM RTKs did not have basal activity in these cell types. Notably, RXDX-106 increased recruitment of T and NK cells into the tumor from both WT and AMdKO backgrounds and increased proliferation of both WT and KO CD8⁺ T cells, indicating that those cell types could be activated indirectly by RXDX-106 (Fig. 5L). RXDX-106 likely cannot directly affect T cells because it did not have a significant impact in *in vitro* T-cell proliferation cultures (Supplementary Fig. S5B and S5C). Interestingly, in the mixed bone marrow chimera setting, MHCII was increased in both AMdKO and WT DCs and macrophages, suggesting that RXDX-106 also had cell-extrinsic effects on the myeloid lineage (in addition to cell-intrinsic role of TAM RTKs at the basal level in these cells). In contrast, this increase in MHCII was not observed in macrophages and DCs from mice reconstituted with complete bone marrow from AMdKO (Fig. 2I; Supplementary Fig. S5D), showing that RXDX-106 directly affected at least these cell types. These also suggest that RXDX-106 affects antigen presentation in the TME, which might be one reason for increased T-cell proliferation and TGI. Altogether, we conclude that RXDX-106 acts directly on WT macrophages and DCs in the chimeric setting, resulting in additional indirect effects on KO immune cells, including myeloid and lymphoid lineages.

RXDX-106 in combination with adaptive immune checkpoint inhibitors

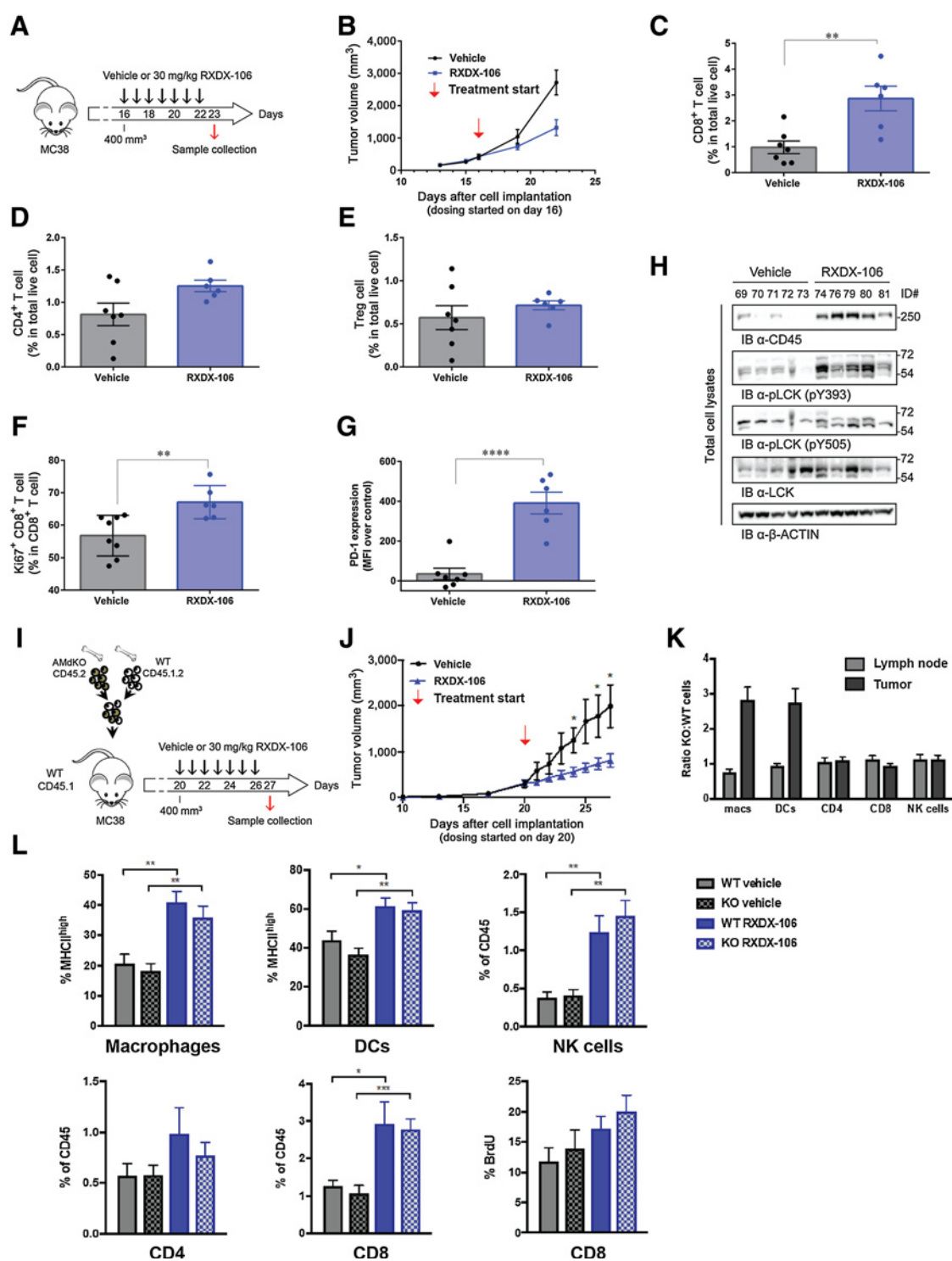
We observed that RXDX-106 led to TGI by activation of both innate and adaptive cells, but the response remains partial (typically <60%). Notably, we found that PD-1 expression on CD8⁺ cells was markedly increased (Fig. 5G; Supplementary Fig. S4E). Therefore, we evaluated the antitumor activity of RXDX-106 in combination with an anti-PD-1Ab in MC38 (Fig. 6A and B) and CT26 (Fig. 6C and D) syngeneic mouse models. In the MC38 model, animals treated with RXDX-106 alone or anti-PD-1Ab displayed similar TGI (TGI = 56% and 66% at day 17, respectively; Fig. 6A), but when given in combination, significantly enhanced TGI was observed (TGI = 86%). Median survival was also enhanced from 17 days (vehicle), to 24, 24, and 28 days for vehicle + anti-PD-1Ab, RXDX-106 alone, and combination, respectively (Fig. 6B, $P = 0.003$, 0.003, and <0.0001, respectively). Similarly, in the CT26 model, RXDX-106 alone and anti-PD-1Ab displayed similar TGI (TGI = 44% and 43% at day 25, respectively; Fig. 6C), although combination of RXDX-106 and anti-PD-1Ab showed significantly enhanced TGI (76%). In addition, survival was significantly enhanced. Median survival of vehicle, vehicle + anti-PD-1Ab, RXDX-106 alone, and combination were 25, 28, 28, and 36.5 days, respectively (Fig. 6D).

To dissect how the combination treatment increased overall survival, RNA-seq analysis was performed in the MC38 model on whole tumors 7 days posttreatment with vehicle or RXDX-106 \pm

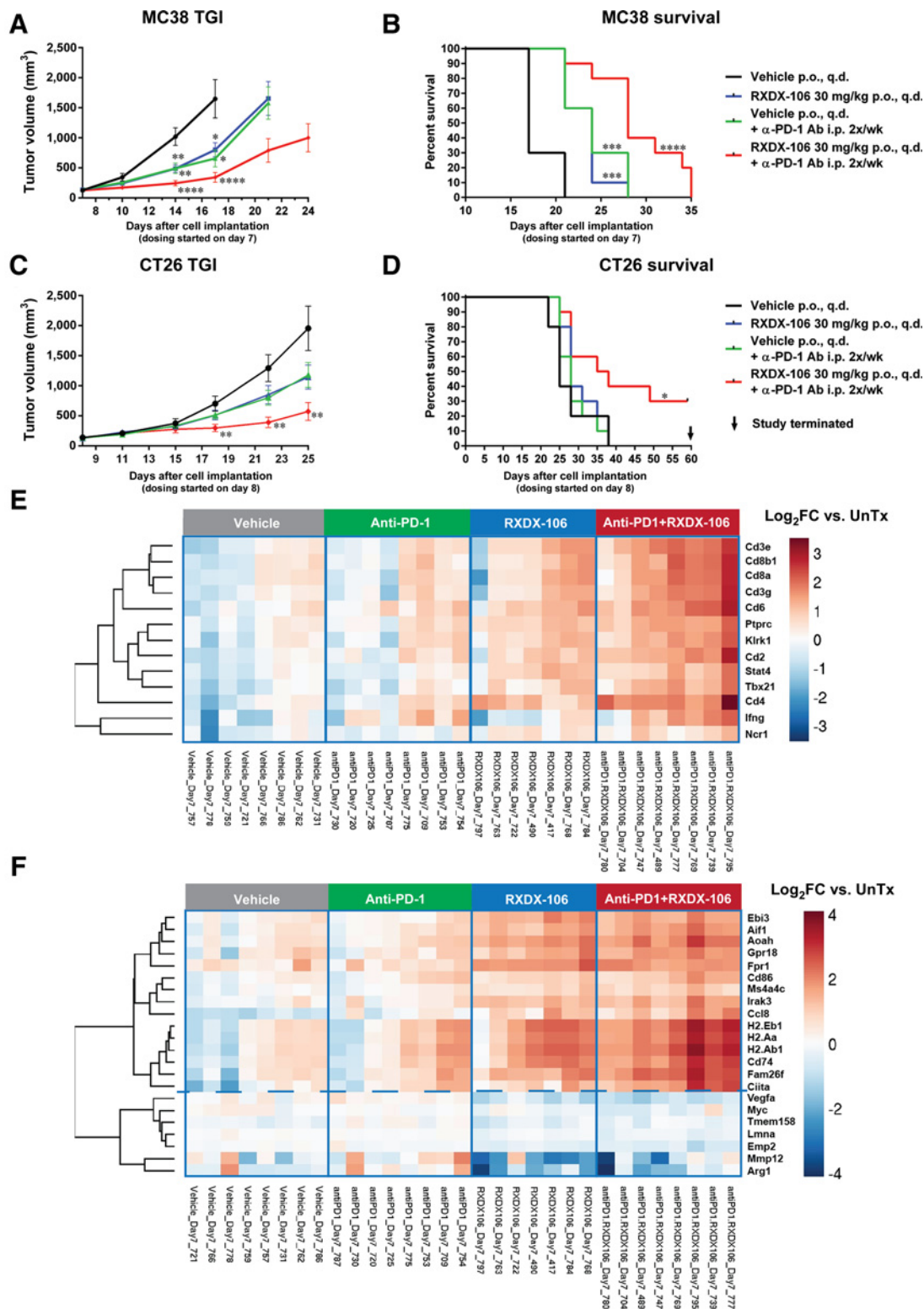
**Figure 4.**

RXDX-106 modulates the innate immune response and induces antitumoral immune response. **A** and **B**, Treatment began when average MC38 tumor size reached 400 mm³ (day 11), and immunophenotyping was performed on day 18 (24 hours posttreatment). **C–K**, Tumor-infiltrating leukocytes (TILs-CD45⁺; **C**), TAM ϕ -CD11b^{hi}Ly6G^{lo}Ly6C^{lo}F4/80^{hi} (**D**), MHCII^{hi} macrophages (M1-like; **E**), MHCII^{lo} macrophages (M2-like; **F**), M1/M2 ratio (**G**), tumor-infiltrating NK-NK1.1⁺ CD335⁺ (**H**), intracellular IFN γ expression by NK cells \pm IL12/IL18/anti-NK1.1Ab re-stimulation (**I**), F4/80⁺ macrophages (**J**), and CD49b⁺ NK cells (**K**) were enriched from RXDX-106-treated, MC38-derived tumors. RT-qPCR analysis was performed 7 days posttreatment. Fold changes (blue, up; red, down) were normalized to a control gene (18S rRNA) and are expressed relative to vehicle; $n = 5$ mice/group. **L** and **M**, Intracellular IFN γ expression in CD8⁺ (**L**) or CD4⁺ (**M**) T cells derived from MC38-dissociated tumors \pm anti-CD3 ϵ /CD28Ab. **N**, ELISA of IFN γ secretion in dissociated tumors \pm anti-CD3 ϵ /CD28Ab restimulation for 3 days; $n = 8$ –10. Data are mean \pm SEM; $n = 8$ –10. *, $P < 0.05$; ***, $P < 0.001$; ****, $P < 0.0001$.

Yokoyama et al.

**Figure 5.**

RXDX-106 indirectly enhances adaptive immune responses by affecting innate immune cells. MC38 cells were inoculated at 1×10^5 cells/mouse so that tumor growth occurred over a longer time period. **A** and **B**, Treatment began when average tumor size reached 400 mm³/day 16, and immunophenotyping was performed on day 23 (24 hours post-treatment). **C–G**, Tumor-infiltrating CD8⁺ (**C**), CD4⁺ (**D**), Treg- (CD25⁺FoxP3⁺) (**E**), Ki67⁺CD8⁺ cells (**F**), PD-1 (**G**) expression on CD8⁺ T cells; $n = 10$. **H**, Western blot analysis of whole tumors containing tumor and immune cells. **I** and **J**, Irradiated CD45.1 WT mice were reconstituted with a 1:1 mixture of CD45.2 WT cells:CD45.1.2 AMdKO cells, challenged with MC38, and treated. Mice were intraperitoneally injected with 1 mg/mouse BrdU 48 and 24 hours before harvest. **K**, Ratios of AMdKO:WT in LNs and tumors. **L**, Percentages of MHCII^{high} macrophages and DCs, NK, CD4⁺, and CD8⁺ T cells of CD45⁺ and BrdU incorporation of CD8⁺ T cells in the tumors; $n = 7$. Data are mean \pm SEM. *, $P < 0.05$; **, $P < 0.01$; ***, $P < 0.001$; ****, $P < 0.0001$.

**Figure 6.**

RXDX-106 potentiates adaptive checkpoint inhibitors in multiple syngeneic models. *In vivo* efficacy of RXDX-106 in combination with anti-PD-1 antibody in MC38 (**A** and **B**) and CT26 (**C** and **D**) models (TGI: **A** and **C**; Survival: **B** and **D**; TGI-ANOVA; Survival-Mantel Cox test). **E** and **F**, Heat maps representing gene level expression of general immune cell markers (**E**) and genes implicated in M1/MHCI^{hi} or M2 macrophage phenotypes (**F**) modulated relative to untreated controls, at a significance level of FDR < 0.01 and log₂ FC > 1. *n* = 8–10 mice/group. Data are representative of two independent experiments. *, *P* < 0.05; **, *P* < 0.01; ***, *P* < 0.001; ****, *P* < 0.0001.

anti-PD-1 antibody. Depicted are heatmaps representing gene-level expression of individual genes that transcribe general immune cell markers (Fig. 6E), and genes previously implicated in M1/MHCII high or M2 macrophage phenotypes (Fig. 6F; refs. 39, 40). Unbiased analysis of all animals showed combination of RXDX-106 and anti-PD-1Ab increased T- and NK-cell-related genes including genes indicating activation, such as *Tbx21*, *Stat4*, *Ifng*, *Klrl1* compared with single-agent treatments. Among genes expressed in macrophages, MHCII-related genes, *Cd86*, and *Ccl8* were increased and M2 macrophage-related genes, such as *Arg1* and *Vegfa*, were decreased in combination group. The increases in immune activation and macrophage polarization observed previously in either the RXDX-106 alone and anti-PD-1Ab-treated groups was further enhanced in combination (Supplementary Table S6), supporting the hypothesis that RXDX-106 would act cooperatively with an adaptive checkpoint inhibitor.

Discussion

The TAM RTKs are emerging targets for cancer therapy as traditional oncogenes and in immuno-oncology as key negative regulators of the innate immune response. Upregulation of TAM RTKs on cancer cells has been well documented, particularly as a mechanism of resistance to both chemotoxic agents and other TKIs and in the maintenance of EMT (14, 41, 42). Furthermore, recent evidence suggests compensatory upregulation of TAM RTK family members (i.e., MER) in response to selective TAM RTK inhibition such as with AXL-specific inhibitors (BGB324; ref. 26) and suggests that selective TAM RTK inhibition relative to pan-TAM RTK inhibition may have limited clinical benefit. Notably, the expression of TAM RTKs and c-MET in syngeneic tumor cell lines is often quite low (Supplementary Fig. S6A–S6D). In the context of the immune system, TAM RTKs are widely expressed on macrophages, DCs, MDSCs, NK, and T cells (16, 28, 43), and can inhibit tumor immunity. Here we demonstrate that expression of AXL and MER on immune and tumor cells increased during tumor progression, supporting development of RXDX-106 as a pan-TAM RTK inhibitor for cancer immunotherapy.

In an activity-based kinase screen, we found that RXDX-106 was highly specific for TAM RTKs with additional activity against c-MET/RON kinase families. Although off-target activity against LCK was observed in the *in vitro* biochemical assay, we did not observe any evidence of *in vivo* inhibition. In fact, tumor-bearing mice treated with RXDX-106 had increased LCK phosphorylation/activation (pY393), leading to increased T-cell activation *in vivo*, trending toward increased proliferation. When compared with other TAM inhibitors currently tested in preclinical or clinical settings, RXDX-106 had slower dissociation kinetics relative to BGB324 (AXL-specific), cabozantinib (c-MET/AXL), or merestinib (MST1R, FLT3, AXL, MERTK, TEK, ROS1, NTRK1/2/3, and DDR1/2, and MKNK1/2), which may translate to more durable target engagement and *in vivo* efficacy.

TAM RTK single, double, and triple knockout mice have been generated and are completely viable with no obvious developmental defects (18). However, the receptors play key homeostatic roles in the clearance of $>10^9$ apoptotic cells daily and particularly, *Mertk*^{-/-} and TAM TKO mice progressively develop a plethora of phenotypes due to the inability of specialized phagocytes like Sertoli and RPE cells in the testes and eye, respectively, to clear PtdSer-expressing apoptotic cells/debris (11, 44, 45). RXDX-106

inhibited AXL and MER-dependent phagocytosis *in vitro* and *in vivo*, but we did not observe accumulation of apoptotic neutrophils in peripheral blood or indications of global autoimmunity (Supplementary Fig. S4F). In addition, tumor growth in WT mice transplanted with AMdKO BM cells was not decreased compared with mice transplanted with WT BM cells and the hyperactivation of immune cells was not seen in the TME, indicating that the intrinsic hyperactivated immune system of those mice was insufficient to inhibit tumor growth.

In addition to their role in phagocytosis, TAM RTKs function to negatively regulate the magnitude and duration of the innate immune response. In response to pathogens, AXL is upregulated and activated downstream of the TLR where it coopts IFNAR1 to induce SOCS1/3 signaling (16). The importance of the TAM RTKs in regulating the immune response is exemplified by the broad-spectrum autoimmunity observed in the TAM TKO mice, which have increased autoantibodies, enlarged lymph nodes, and splenomegaly (18). In addition, TAM RTKs on NK cells may promote tumor growth and metastasis via negatively regulating NK-mediated antitumor response, a process that requires both the kinase activity and Cbl-mediated internalization (28). In this report, we demonstrate that RXDX-106 significantly increased infiltration of immune cells into tumors (TIL) and augmented both innate and adaptive immune responses. Using bone marrow chimeric mice reconstituted with a mixture of WT and AMdKO cells, we found that RXDX-106 directly activated macrophages and DCs (derived from WT BM) but also indirectly activated macrophages, DCs, NK cells, CD4⁺ and CD8⁺ T cells (derived from AMdKO BM). This indirect activation likely resulted from increased antigen presentation and polarization of the innate response toward an M1-like state. We also showed that the global activation of immunity by RXDX-106 required AXL and MER because we did not observe these effects in RXDX-106-treated AMdKO BM macrophages and DCs in nonchimeric bone marrow-reconstituted animals (that lacked WT cells that could respond to RXDX-106).

Recent reports suggest that c-MET can also play a role in mitigating the immune response due to its expression on neutrophils in the context of adoptive T-cell transfer immunotherapy (46). Although RXDX-106 is 7-fold more potent against the TAM RTK family, we cannot rule out the possibility that RXDX-106 may exert a minimal immunomodulatory effect through c-MET. However, it is unlikely because we observed no TGI after RXDX-106 treatment in mice transplanted with AMdKO BM that still express c-MET. In addition, we did not observe changes in neutrophil number in either the TME or peripheral blood (Supplementary Fig. S4F), and only minimal expression of c-MET on tumor cells was observed in cell lines utilized. Because RXDX-106 did not decrease tumor growth in mice that had AMdKO immune cells, we conclude that its antitumor activity is solely mediated by AXL and MER on immune cells, not by TYRO3 or another kinase. It is unclear whether AXL, MER, or both need to be inhibited for our effects. Other studies have found that inhibiting MER alone using UNC2025 led to tumor regression but did not fully examine effects on immunity (47–49), in part, due to use of xenograft models. BGB324, a specific AXL inhibitor in clinical trials, has also demonstrated efficacy in the treatment of various cancers and also shows immune-activating activity (50, 51).

In the TME, RXDX-106 suppressed both transcript and protein levels of VEGF. In the TME, macrophages, MDSCs, and tumor cells are considered to be the major sources of VEGF. We believe that

RXDX-106 reduced VEGF production by tumor cells, at least as the inciting event because: (i) reduction of VEGF protein in tumors was observed at a lower dose (1 mg/kg) and at an earlier time point (day 3) compared with the induction of M1 polarization of macrophages by RXDX-106 (>30 mg/kg and at day 5–9); (ii) there was no noticeable change in the MDSCs in tumors of RXDX-106 treated mice (Supplementary Fig. S3E); and (iii) Transcripts for *Vegf* in macrophages were not changed. Nevertheless, M2-like TAM ϕ are known to produce more VEGF than M1-like macrophages (52). Moreover, the interaction between tumor cells and macrophages has been reported to increase VEGF production (53, 54), which in turn also recruits macrophage progenitors that can then differentiate into M2-like macrophages that produce more VEGF (55), creating a positive feedback loop (53, 54). Further studies are required to delineate how TAM RTKs control expression of VEGF in cancer and immune cells.

We also found that RXDX-106 treatment increased T-cell activation (increased *ex vivo* IFN γ production) and increased %CD8⁺ cells. These effects were T-cell–extrinsic because RXDX-106 was able to act on AMDKO T cells in bone marrow chimeras, possibly by acting on WT innate immune cells that in turn activate CD8⁺ T cells. To our knowledge, these studies are the first to demonstrate the role of TAM RTKs in regulating T-cell activity. Whether TAM RTK expression on T cells has additional direct functions still needs to be determined. Interestingly, a previous study from Carrera-Silva and colleagues showed that activated T cells upregulate PROS1 and concomitantly externalize PtdSer. This complex binds to TAM RTKs on APCs and suppresses their activity (17). It is unknown whether this complex is also seen in tumor-infiltrating T cells or whether T cells can present TAM RTK ligands to other T cells.

Using two syngeneic models, RXDX-106 and anti-PD-1 had similar effects but had more significant effects in combination. These results suggest merit in investigating combinations with other immune checkpoint inhibitors and identification of precise mechanisms of action governing observed potentiation.

In summary, RXDX-106 can restore and enhance immune function by modulating the local immune-suppressive TME. The

unique mechanisms of activating both innate and adaptive immunity, and regulating cross-talk between immune and tumor cells, support clinical evaluation of RXDX-106 as an immunomodulatory agent for the treatment of a variety of cancers.

Disclosure of Potential Conflicts of Interest

J.D. Bui reports receiving commercial research grant from Ignyta and is a consultant/advisory board member of Ignyta. No potential conflicts of interest were disclosed by the other authors.

Authors' Contributions

Conception and design: Y. Yokoyama, E.D. Lew, R. Seelige, E.A. Tindall, C. Walsh, J.Y. Lee, K.M. Smith, G. Li, J.D. Bui

Development of methodology: Y. Yokoyama, E.D. Lew, R. Seelige, E.A. Tindall, C. Walsh, P.C. Fagan, J.Y. Lee, H. Vaaler, K.M. Smith, J.D. Bui

Acquisition of data (provided animals, acquired and managed patients, provided facilities, etc.): Y. Yokoyama, E.D. Lew, R. Seelige, C. Walsh, P.C. Fagan, J.Y. Lee, R. Nevarez, J. Oh, K.D. Tucker, M. Chen, H. Vaaler, K.M. Smith, J.D. Bui

Analysis and interpretation of data (e.g., statistical analysis, biostatistics, computational analysis): Y. Yokoyama, E.D. Lew, R. Seelige, E.A. Tindall, C. Walsh, P.C. Fagan, J.Y. Lee, R. Nevarez, J. Oh, K.D. Tucker, A. Diliberto, G. Li, J.D. Bui

Writing, review, and/or revision of the manuscript: Y. Yokoyama, E.D. Lew, R. Seelige, E.A. Tindall, P.C. Fagan, J.Y. Lee, J. Oh, A. Diliberto, H. Vaaler, K.M. Smith, A. Albert, G. Li, J.D. Bui

Administrative, technical, or material support (i.e., reporting or organizing data, constructing databases): Y. Yokoyama, E.D. Lew, E.A. Tindall, P.C. Fagan, J. Oh, K.D. Tucker

Study supervision: Y. Yokoyama, C. Walsh, A. Albert, G. Li, J.D. Bui

Acknowledgments

We thank members of Ignyta and the RXDX-106 team for their support. We also acknowledge Drs. Gloria Hernandez-Torres, Greg Lemke, and Kaisa Happonen for technical assistance and manuscript comments.

The costs of publication of this article were defrayed in part by the payment of page charges. This article must therefore be hereby marked *advertisement* in accordance with 18 U.S.C. Section 1734 solely to indicate this fact.

Received July 2, 2018; revised November 16, 2018; accepted January 30, 2019; published first February 5, 2019.

References

- Korman AJ, Peggs KS, Allison JP. Checkpoint blockade in cancer immunotherapy. *Adv Immunol* 2006;90:297–339.
- Ribas A, Wolchok JD. Cancer immunotherapy using checkpoint blockade. *Science* 2018;359:1350–5.
- Chen Daniel S, Mellman I. Oncology meets immunology: the cancer-immunity cycle. *Immunity* 2013;39:1–10.
- Wei SC, Levine JH, Cogdill AP, Zhao Y, Anang NAS, Andrews MC, et al. Distinct cellular mechanisms underlie anti-CTLA-4 and anti-PD-1 checkpoint blockade. *Cell* 2017;170:1120–33.
- Kumar V, Patel S, Tcyganov E, Gabrilovich DI. The nature of myeloid-derived suppressor cells in the tumor microenvironment. *Trends Immunol* 2016;37:208–20.
- Mantovani A, Sozzani S, Locati M, Allavena P, Sica A. Macrophage polarization: tumor-associated macrophages as a paradigm for polarized M2 mononuclear phagocytes. *Trends Immunol* 2002;23:549–55.
- Cubillos-Ruiz JR, Bettigole SE, Glimcher LH. Molecular pathways: immunosuppressive roles of IRE1 α -XBP1 signaling in dendritic cells of the tumor microenvironment. *Clin Cancer Res* 2016;22:2121–6.
- Costello RT, Sivori S, Marcenaro E, Lafage-Pochitaloff M, Mozziconacci MJ, Reviron D, et al. Defective expression and function of natural killer cell-triggering receptors in patients with acute myeloid leukemia. *Blood* 2002;99:3661–7.
- Corrales L, Matson V, Flood B, Spranger S, Gajewski TF. Innate immune signaling and regulation in cancer immunotherapy. *Cell Res* 2017;27:96–108.
- Akalu YT, Rothlin CV, Ghosh S. TAM receptor tyrosine kinases as emerging targets of innate immune checkpoint blockade for cancer therapy. *Immunol Rev* 2017;276:165–77.
- Scott RS, McMahon EJ, Pop SM, Reap EA, Caricchio R, Cohen PL, et al. Phagocytosis and clearance of apoptotic cells is mediated by MER. *Nature* 2001;411:207–11.
- Lemke G. Phosphatidyserine is the signal for TAM receptors and their ligands. *Trends Biochem Sci* 2017;42:738–48.
- Filardy AA, Pires DR, Nunes MP, Takiya CM, Freire-de-Lima CG, Ribeiro-Gomes FL, et al. Proinflammatory clearance of apoptotic neutrophils induces an IL-12(low)IL-10(high) regulatory phenotype in macrophages. *J Immunol* 2010;185:2044–50.
- Graham DK, DeRyckere D, Davies KD, Earp HS. The TAM family: phosphatidyserine sensing receptor tyrosine kinases gone awry in cancer. *Nat Rev Cancer* 2014;14:769–85.
- Fadok VA, Bratton DL, Konowal A, Freed PW, Westcott JY, Henson PM. Macrophages that have ingested apoptotic cells in vitro inhibit proinflammatory cytokine production through autocrine/paracrine mechanisms involving TGF- β , PGE2, and PAF. *J Clin Invest* 1998;101:890–8.

16. Rothlin CV, Ghosh S, Zuniga EI, Oldstone MB, Lemke G. TAM receptors are pleiotropic inhibitors of the innate immune response. *Cell* 2007;131:1124–36.
17. Carrera Silva EA, Chan PY, Joannas L, Errasti AE, Gagliani N, Bosurgi L, et al. T cell-derived protein S engages TAM receptor signaling in dendritic cells to control the magnitude of the immune response. *Immunity* 2013;39:160–70.
18. Lu Q, Lemke G. Homeostatic regulation of the immune system by receptor tyrosine kinases of the Tyro 3 family. *Science* 2001;293:306–11.
19. Graham DK, Dawson TL, Mullaney DL, Snodgrass HR, Earp HS. Cloning and mRNA expression analysis of a novel human protooncogene, *c-mer*. *Cell Growth Differ* 1994;5:647–57.
20. Lee-Sherick AB, Eisenman KM, Sather S, McGranahan A, Armistead PM, McGary CS, et al. Aberrant Mer receptor tyrosine kinase expression contributes to leukemogenesis in acute myeloid leukemia. *Oncogene* 2013;32:5359–68.
21. Linger RM, Cohen RA, Cummings CT, Sather S, Migdall-Wilson J, Middleton DH, et al. Mer or Axl receptor tyrosine kinase inhibition promotes apoptosis, blocks growth and enhances chemosensitivity of human non-small cell lung cancer. *Oncogene* 2013;32:3420–31.
22. McCloskey P, Pierce J, Koski R, Varnum B, Liu E. Activation of the Axl receptor tyrosine kinase induces mitogenesis and transformation in 32D cells. *Cell Growth Differ* 1994;5:1105–17.
23. Shiozawa Y, Pedersen EA, Patel LR, Ziegler AM, Havens AM, Jung Y, et al. GAS6/AXL axis regulates prostate cancer invasion, proliferation, and survival in the bone marrow niche. *Neoplasia* 2010;12:116–27.
24. Brandao LN, Wings A, Christoph S, Sather S, Migdall-Wilson J, Schlegel J, et al. Inhibition of MerTK increases chemosensitivity and decreases oncogenic potential in T-cell acute lymphoblastic leukemia. *Blood Cancer J* 2013;3:e101.
25. Lemke G, Rothlin CV. Immunobiology of the TAM receptors. *Nat Rev Immunol* 2008;8:327–36.
26. McDaniel NK, Cummings CT, Iida M, Hulse J, Pearson HE, Vasileiadis E, et al. MERTK mediates intrinsic and adaptive resistance to AXL-targeting agents. *Mol Cancer Ther* 2018;17:2297–308.
27. Rankin EB, Giaccia AJ. The receptor tyrosine kinase AXL in cancer progression. *Cancers* 2016;8:103.
28. Paolino M, Choidas A, Wallner S, Pranjic B, Uribealago I, Loeser S, et al. The E3 ligase Cbl-b and TAM receptors regulate cancer metastasis via natural killer cells. *Nature* 2014;507:508–12.
29. Seitz HM, Camenisch TD, Lemke G, Earp HS, Matsushima GK. Macrophages and dendritic cells use different Axl/Mertk/Tyro3 receptors in clearance of apoptotic cells. *J Immunol* 2007;178:5635–42.
30. Zagórska A, Través PG, Lew ED, Dransfield I, Lemke G. Diversification of TAM receptor tyrosine kinase function. *Nat Immunol* 2014;15:920.
31. Vijayan RSK, He P, Modi V, Duong-Ly KC, Ma H, Peterson JR, et al. Conformational analysis of the DFG-Out kinase motif and biochemical profiling of structurally validated type II inhibitors. *J Med Chem* 2015;58:466–79.
32. Copeland RA. The drug–target residence time model: a 10-year retrospective. *Nat Rev Drug Discov* 2015;15:87.
33. Lew ED, Oh J, Burrola PG, Lax I, Zagórska A, Través PG, et al. Differential TAM receptor–ligand–phospholipid interactions delimit differential TAM bioactivities. *eLife* 2014;3:e03385.
34. Linger RM, Keating AK, Earp HS, Graham DK. TAM receptor tyrosine kinases: biologic functions, signaling, and potential therapeutic targeting in human cancer. *Adv Cancer Res* 2008;100:35–83.
35. O'Bryan JP, Frye RA, Cogswell PC, Neubauer A, Kitch B, Prokop C, et al. *axl*, a transforming gene isolated from primary human myeloid leukemia cells, encodes a novel receptor tyrosine kinase. *Mol Cell Biol* 1991;11:5016–31.
36. Holtzhausen A, Harris WT, Hunter D, Ubil E, Wang X, Graham DK, et al. TAM RTK inhibition enhances anti-tumor T cell responses by reversing MDSC-mediated suppression. 32nd Annual Meeting and Pre-Conference Programs of the Society for Immunotherapy of Cancer (SITC 2017): Part Two. *J Immuno Ther Cancer* 2017;5(Suppl 2):P463. doi: 10.1186/s40425-017-0288-4.
37. Cabezon R, Carrera-Silva EA, Florez-Grau G, Errasti AE, Calderon-Gomez E, Lozano JJ, et al. MERTK as negative regulator of human T cell activation. *J Leukoc Biol* 2015;97:751–60.
38. Schmid ET, Pang IK, Carrera Silva EA, Bosurgi L, Miner JJ, Diamond MS, et al. AXL receptor tyrosine kinase is required for T cell priming and antiviral immunity. *Elife* 2016;5:pii: e12414.
39. Jablonski KA, Amici SA, Webb LM, Ruiz-Rosado JdD, Popovich PG, Partida-Sanchez S, et al. Novel markers to delineate murine M1 and M2 Macrophages. *PLoS ONE* 2015;10:e0145342.
40. Mosely SIS, Prime JE, Sainson RCA, Koopmann J-O, Wang DYQ, Greenawalt DM, et al. Rational selection of syngeneic preclinical tumor models for immunotherapeutic drug discovery. *Cancer Immunol Res* 2017;5:29–41.
41. Linger RMA, Cohen RA, Cummings CT, Sather S, Migdall-Wilson J, Middleton DHG, et al. Mer or Axl receptor tyrosine kinase inhibition promotes apoptosis, blocks growth, and enhances chemosensitivity of human non-small cell lung cancer. *Oncogene* 2013;32:3420–31.
42. Zhang Z, Lee JC, Lin L, Olivas V, Au V, LaFramboise T, et al. Activation of the AXL kinase causes resistance to EGFR-targeted therapy in lung cancer. *Nat Genet* 2012;44:852–60.
43. Davra V, Kimani SG, Calianese D, Birge RB. Ligand activation of TAM family receptors-implications for tumor biology and therapeutic response. *Cancers* 2016;8:pii: E107.
44. Lu Q, Gore M, Zhang Q, Camenisch T, Boast S, Casagrande F, et al. Tyro-3 family receptors are essential regulators of mammalian spermatogenesis. *Nature* 1999;398:723.
45. Burstyn-Cohen T, Lew Erin D, Través Paqui G, Burrola Patrick G, Hash Joseph C, Lemke G. Genetic dissection of TAM receptor-ligand interaction in retinal pigment epithelial cell phagocytosis. *Neuron* 2012;76:1123–32.
46. Glodde N, Bald T, van den Boorn-Konijnenberg D, Nakamura K, O'Donnell JS, Szczepanski S, et al. Reactive neutrophil responses dependent on the receptor tyrosine kinase c-MET limit cancer immunotherapy. *Immunity* 2017;47:789–802.
47. Wu J, Frady LN, Bash RE, Cohen SM, Schorzman AN, Su Y-T, et al. MerTK as a therapeutic target in glioblastoma. *Neuro-Oncol* 2018;20:92–102.
48. DeRyckere D, Lee-Sherick AB, Huey MG, Hill AA, Tyner JW, Jacobsen KM, et al. UNC2025, a MERTK small molecule inhibitor, is therapeutically effective alone and in combination with methotrexate in leukemia models. *Clin Cancer Res* 2017;23:1481–92.
49. Cummings CT, Zhang W, Davies KD, Kirkpatrick GD, Zhang D, DeRyckere D, et al. Small molecule inhibition of MERTK is efficacious in non-small cell lung cancer models independent of driver oncogene status. *Mol Cancer Ther* 2015;14:2014–22.
50. Sadahiro H, Kang K-D, Gibson JT, Minata M, Yu H, Shi J, et al. Activation of the receptor tyrosine kinase AXL regulates the immune microenvironment in glioblastoma. *Cancer Res* 2018;78:3002–13.
51. Ludwig KF, Du W, Sorrelle NB, Wnuk-Lipinska K, Topalovski M, Toombs JE, et al. Small-molecule inhibition of axl targets tumor immune suppression and enhances chemotherapy in pancreatic cancer. *Cancer Res* 2018;78:246–55.
52. Lin EY, Pollard JW. Tumor-associated macrophages press the angiogenic switch in breast cancer. *Cancer Res* 2007;67:5064–6.
53. Liu XQ, Kiehl R, Roskopf C, Tian F, Huber RM. Interactions among lung cancer cells, fibroblasts, and macrophages in 3D co-cultures and the impact on MMP-1 and VEGF expression. *PLoS One* 2016;11:e0156268.
54. Hagemann T, Wilson J, Burke F, Kulbe H, Li NF, Pludemann A, et al. Ovarian cancer cells polarize macrophages toward a tumor-associated phenotype. *J Immunol* 2006;176:5023–32.
55. Linde N, Lederle W, Depner S, van Rooijen N, Gutschalk CM, Mueller MM. Vascular endothelial growth factor-induced skin carcinogenesis depends on recruitment and alternative activation of macrophages. *J Pathol* 2012;227:17–28.

Cancer Research

The Journal of Cancer Research (1916–1930) | The American Journal of Cancer (1931–1940)

Immuno-oncological Efficacy of RXDX-106, a Novel TAM (TYRO3, AXL, MER) Family Small-Molecule Kinase Inhibitor

Yumi Yokoyama, Erin D. Lew, Ruth Seelige, et al.

Cancer Res 2019;79:1996-2008. Published OnlineFirst February 5, 2019.

Updated version Access the most recent version of this article at:
doi:[10.1158/0008-5472.CAN-18-2022](https://doi.org/10.1158/0008-5472.CAN-18-2022)

Supplementary Material Access the most recent supplemental material at:
<http://cancerres.aacrjournals.org/content/suppl/2019/02/05/0008-5472.CAN-18-2022.DC1>

Cited articles This article cites 55 articles, 16 of which you can access for free at:
<http://cancerres.aacrjournals.org/content/79/8/1996.full#ref-list-1>

E-mail alerts [Sign up to receive free email-alerts](#) related to this article or journal.

Reprints and Subscriptions To order reprints of this article or to subscribe to the journal, contact the AACR Publications Department at pubs@aacr.org.

Permissions To request permission to re-use all or part of this article, use this link
<http://cancerres.aacrjournals.org/content/79/8/1996>.
Click on "Request Permissions" which will take you to the Copyright Clearance Center's (CCC) Rightslink site.